SURFACE STABILITY OF AN ENCAPSULATED BUBBLE IN AN ULTRASOUND FIELD

Yunqiao Liu*[a)], Kazuyasu Sugiyama** Shu Takagi**& Yoichiro Matsumoto**
*Department of Engineering Mechanics, Shanghai Jiao Tong University, Shanghai, 200240, China
**Department of Mechanical Engineering, School of Engineering, The University of Tokyo, 7-3-1 Hongo, Bunkyo-ku, Tokyo 113-8656, Japan

Summary In this paper, we investigate the shape stability of a nearly spherical bubble encapsulated by a viscoelastic membrane in an ultrasound field. To describe the dynamic balance on the bubble surface, the in-plane stress and the bending moment are incorporated into the governing equations for the perturbed radial flow of viscous incompressible fluid (Prosperetti (1977) *Quart. Appl. Math.*, **35**, 339). The radial motion of the bubble is obtained by solving the Rayleigh-Plesset equation with elastic stress. The deflection therefrom is linearized and expanded with respect to the Legendre polynomial of order $k \geq 2$. Two amplitudes for each shape mode are introduced because the membrane moves not only in the radial direction but also in the tangential direction. Stability diagrams for the higher-order shape mode are mapped out in the phase space of driving amplitude and frequency over a range of values of the elastic modulus of the membrane. The most unstable driving frequency is found to satisfy an integer multiple relationship of the form $2\omega_k/\omega_d = n$, due to the structure of Mathieu's equation in the system.

PROBLEM FORMULATION

We consider a single bubble suspended in an unbounded acoustic field. The driving pressure applied from the far field is characterized by a sinusoidal wave with a dimensionless amplitude ε and a driving frequency ω_d. The governing equations for the external flow field are the continuity equation and the incompressible Navier-Stokes equation. The gas pressure inside the bubble is assumed to vary according to the polytropic process. Different from the gas bubble, the bubble encapsulated by a membrane bears a no-slip condition at the surface. The dynamic equilibrium at the bubble surface is described by a traction jump across the membrane. The membrane stress is given by the surface divergence of the elastic tension tensor. We consider a viscoelastic membrane, which exhibits both viscous and elastic characteristics. The constitutive law of the elastic part is described by the neo-Hookean law.
For an encapsulated bubble the material points move along the interface since the membrane bears in-plane stresses. For this reason, we must consider the motion in the tangential direction. Furthermore, the viscous effect is significant for a small bubble with micrometer size. And due to the no-slip condition, the vorticity induced by deformation will influence the dynamics of the bubble and thus cannot be neglected. Therefore, instead of potential flow theory, which is inadequate for describing the frictional traction jump, we employ the theory by [1] that includes a viscous correction to Plesset's potential model [2].

Dynamic balances at encapsulating membrane

We summarize the derived equations about dynamic balances at the encapsulating membrane in the following. The radial motion is determined by

$$R\ddot{R} + \frac{3}{2}\dot{R}^2 + \frac{1}{\rho}\Big[\frac{2\gamma}{R} + 4\mu_l\frac{\dot{R}}{R} - p_g + p_\infty + \frac{2G_s(R^6-R_0^6)}{R^7} + 4\mu_s\frac{\dot{R}}{R^2}\Big] = 0. \tag{1}$$

The dynamics of shape modes is

$$\begin{aligned}
&\frac{\rho R}{k+1}\ddot{a}_k + \Big[\frac{3\rho}{k+1}\dot{R} - \frac{2\mu_l(k+2)(k-1)}{R}\Big]\dot{a}_k \\
&+\Big[-\frac{k-1}{k+1}\rho\ddot{R} + 2\mu_l(k-1)(k+2)\frac{\dot{R}}{R^2} + (k-1)(k+2)\frac{\gamma}{R^2}\Big]a_k + \mu_l k(k+2)\frac{T(R,t)}{R} \\
&+k\rho\frac{\dot{R}}{R}\int_R^\infty[(R/s)^3-1](R/s)^k T(s,t)ds + \frac{G_s(k-1)(k+2)}{R^8}\big[(R^6-7R_0^6)a_k + k(k+1)(3R_0^6+R^6)b_k\big] \\
&+\frac{2\mu_s(k-1)(k+2)}{R^3}\big[(2a_k\dot{R} - R\dot{a}_k) + k(k+1)(R\dot{b}_k - \dot{R}b_k)\big] = 0,\ k\geq 2.
\end{aligned} \tag{2}$$

The tangential dynamic balance is

$$\begin{aligned}
&\mu_l\Big[(2k+4)\frac{\dot{a}_k}{R} - (2k-2)\frac{a_k\dot{R}}{R^2} - (k+1)\frac{T(R,t)}{R} + (4k+2)R^{k-2}\alpha(t)\Big] \\
=\ &\frac{G_s(k+1)}{R^8}\{(R^6-7R_0^6)a_k + [3k(k+1)R_0^6 + (k-1)(k+2)R^6]b_k\} \\
&+\frac{G_b}{R^4}(k+1)(k^2+k-1+\upsilon)(b_k-a_k) + \frac{2\mu_s(k+1)}{R^3}\big[2\dot{R}a_k - R\dot{a}_k + (k^2+k-1)(R\dot{b}_k - \dot{R}b_k)\big].
\end{aligned} \tag{3}$$

[a)] Corresponding author. E-mail: yunqiaoliu@sjtu.edu.cn

In the above equations, R is the radial variance; a_k and b_k are the amplitudes of disturbance at k-th order shape mode in radial and tangential directions, respectively; G_s, G_b and μ_s are the elastic modulus, bending modulus and membrane viscosity, respectively. $T(r,t)$ is the toroidal field, solved by

$$\rho\frac{\partial T}{\partial t}+\rho\frac{\partial}{\partial r}[\dot{R}(R/r)^2T]-\mu_l\frac{\partial^2 T}{\partial r^2}+\mu_l k(k+1)r^{-2}T=0. \tag{4}$$

Tangential velocity boundary condition

We employ a no-velocity-jump condition:

$$\dot{b}_k-\frac{\dot{R}}{R}b_k=-\frac{\dot{a}_k+\frac{2\dot{R}a_k}{R}}{k+1}+R^{k-1}\int_R^\infty s^{-k}T(s,t)ds. \tag{5}$$

STABILITY DIAGRAM

Figure 1 illustrates the phase diagram of shape stabilities of the five encapsulated bubbles, and that of the gas bubble. The phase diagram is plotted as a function of the driving frequency normalized by the second-order natural frequency ω_d/ω_2 and the thresholds of the driving pressure amplitude ε. The curves in Figure 1 represent the borderlines of stability, above which the shape oscillations become unstable, while below which the surface instabilities do not occur. Generally speaking, the oscillations behave in a more stable way above resonance than below resonance. For extremely high driving frequency, a strong driving pressure is needed to induce the shape modes. This is understandable because under high driving frequency, the oscillatory period is so short that the surface instability has insufficient time in which to develop. Most significantly, it is found that minima appear in the vicinity of $\omega_d/\omega_2 = 2$ for all of the encapsulated and gas bubbles, and secondary minima emerge in the neighborhood of $\omega_d/\omega_2 = 1$. These unstable situations can be explained by the structure of Mathieu's equation embedded in the system, which are the so-called one-two resonance and one-one resonance.

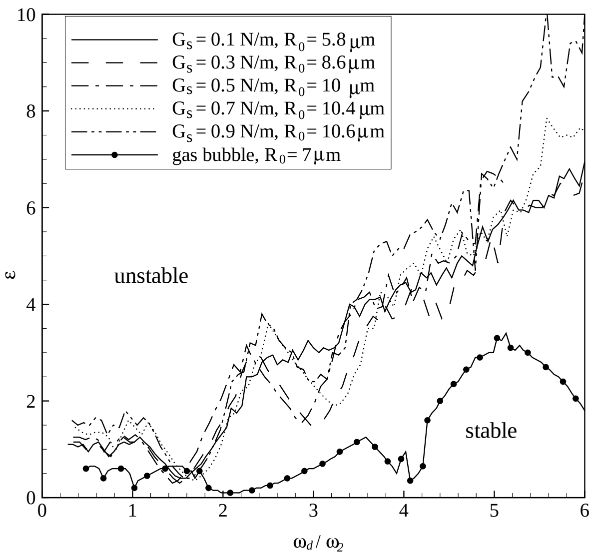

Figure 1. Stability diagram of 2nd-order shape mode.

CONCLUSIONS

We have derived the equations for the shape oscillation of an encapsulated bubble. The membrane stress and bending moment are coupled into the traction jump condition at the bubble surface. Due to the no-slip condition at the membrane, the movement of the material points along the surface, as well as their surface-normal motion, is considered. The non-spherical shape instability is investigated in the context of a viscous incompressible fluid. The derived system bears the structure of Mathieu's equation, which predicts the stability condition of $2\omega_k/\omega_d = n$, where n is an integer. The stability diagrams of the higher-order shape modes validates the unstable condition.

References

[1] Prosperetti A.: Viscous effects on perturbed spherical flows. *Q. Appl. Maths* **34**:339–352, 1977.

[2] Plesset, M.S.: On the stability of fluid flows with spherical symmetry. *J. Appl. Phys.* **25**:96–98, 1954.